POD & MLSM Application on DU96-W180 Wind Turbine Airfoil

Halawa, Amr M.
Interdisciplinary Graduate School of Engineering Sciences, Kyushu University | Department of Aerospace Engineering, Cairo University

Elhadidi, Basman
School of Mechanical & Aerospace Engineering, Nanyang Technological University

Yoshida, Shigeo
Research Institute for Applied Mechanics, Kyushu University

https://doi.org/10.5109/1808451

出版情報：Evergreen. 4 (1), pp.36-43, 2017-03. 九州大学グリーンアジア国際リーダー教育センター
バージョン：
権利関係：

POD & MLSM Application on DU96-W180 Wind Turbine Airfoil

Amr M. Halawa[1,2,*], Basman Elhadidi[3], Shigeo Yoshida[4]

[1]Interdisciplinary Graduate School of Engineering Sciences, Kyushu University, Japan

[2]Department of Aerospace Engineering, Cairo University, Egypt

[3]School of Mechanical & Aerospace Engineering, Nanyang Technological University, Singapore

[4]Research Institute for Applied Mechanics, Kyushu University, Japan

*Author to whom correspondence should be addressed,

E-mail: amrhalawa@riam.kyushu-u.ac.jp

(Received December 14, 2016; accepted March 1, 2017).

In this study, the aim was to reduce the complexity of the costly non-linear unsteady partial differential equations governing the aerodynamic flows into a simpler lower-dimensional model. Modal decomposition method; namely Proper Orthogonal Decomposition (POD) was applied in conjunction with the Modified Linear Stochastic Measurement (MLSM) to achieve a reduced order model with high accuracy and low computational cost. The methods were applied to the surface pressure values of a DU96-W180 Wind Turbine Airfoil with emphasis on stall control application. It was found that using only three POD modes, most of the system energy (up to 99%) was captured where the reconstructed pressure distribution matched the CFD one obtained from OpenFOAM simulations. Besides, using only two pressure probes, one upstream and the other downstream, the surface pressure field was reconstructed with high accuracy. This application is important in reducing the computational time from several hours to just few seconds for applications involving recursive solution of the Navier-Stokes equations.

Keywords: POD, MLSM, CFD, OpenFOAM.

1. Introduction

Reduced-order models (ROMs) are mainly aiming at capturing detailed knowledge of the physical behavior of flow field via simple, robust, and convenient models. The nature of aerodynamic flows yields non-linear unsteady partial differential equations whose computation requires numerical algorithms to be implemented on parallel massive super-computers which is a very complex task [1]. Thus the essential need arises for other efficient tools to reducing the original complicated system of equations into a simple lower-dimensional model characterizing the physical process and capturing its behavior with relatively smaller number of degrees of freedom and lower computational cost [1]. The computation of a ROM could be done by either numerical simulations or measured experimental data. Those models were successfully applied in various areas like steady analysis and design of inviscid airfoils, thermal chemical processing, and dynamical models [2]. The major contributions in reduced-order modeling are currently focused on unsteady aerodynamics. However, they can be applied to steady aerodynamics applications too.

Lumley [3] was the first to propose Proper Orthogonal Decomposition (POD) in 1967 as a neutral method for the study of coherent structures in turbulent flows. The attractiveness of the POD method lies in the fact that it is a linear procedure [2] and efficient in the design of robust feedback controllers leading to better controlled air flow over airfoils. Afterwards, much computational and experimental work has been done by using this method to validate its effectiveness [4]. To name a few, Siegel et al. in 2004 [5] have showed promising results for POD based feedback control when applied to a laminar flow around a circular cylinder. Moreover, controlling cylinder wake was achieved through POD models in 2006 by Luchtenburg et al [6], Siegel et al [7], and in suppressing the separation over airfoils by Ausseur et al. [8].

On the other hand, Modified Linear Stochastic Measurements (MLSM) method is applied alongside POD method to reconstruct the flow field for the whole domain knowing only one of the variables of the flow field at some few points. Adrian [9] was the first to propose applying linear stochastic estimation (LSE) in 1977 to a set of instantaneous data. He realized that using the instantaneous data information along with the statistical information inside the correlation tensor could yield a method to estimate the flow field. Next, this deduction was interpreted by Cole et al. [10] in the shear layer of an axisymmetric jet in 1991 where using the information

from only few radial locations, the radial velocity across the shear layer of the jet was estimated successfully. Afterwards, the research of Adrian and Cole et al. was expanded in 1994 by Bonnet et al. [11] to a complementary method where both the POD and LSE are combined to get POD's time series coefficients using the instantaneous data of the velocity that was measured on coarse grids of hot wire. This method was formerly called the Modified Linear Stochastic Estimation (MLSE), but later renamed to Modified Linear Stochastic Measurement so as to distinguish between the actual measurement technique being done in this case and the estimation process usually associated with a plant estimation in control applications community.

Recent applications of POD/MLSM by Schmit and Glauser in 2003 [12] and 2004 [13] to the wake flow for the wing of a Micro Air Vehicle (MAV) shows the validity of MLSM to external flows applications. They mounted dynamic strain gages on their MAV's flexible wing and was able to reconstruct the wake velocity field with reasonable accuracy. Moreover, Glauser et al. [14] showed in 2004 that a POD/MLSM technique could reasonably estimate the velocity field over NACA-4412 airfoil from only the information given by pressure sensors at the surface of the airfoil. Besides, in 2009, El-Desouky [15] applied the POD/MLSM technique to control the unsteady Kármán vortex shedding for a circular cylinder and was able to achieve over 96% of the system energy using only 4 modes.

2. Proper orthogonal decomposition

Simply, an eigenvalue problem needs to be solved. A linear system is formed from the eigenfunctions that can be computed from a set of data extracted from the system. Using a mathematical approach that is based on the Karhunen-Loeve decomposition in which any field variable is decomposed into a finite number of empirical orthogonal eigenfunctions derived from the set of the readings and are chosen to maximize their mean square projection onto the field variable. Thus, POD optimally describes the energy content in the flow using the minimum number of eigenfunctions [4]. The procedure that is followed here is similar to the work of El-Desouky [15]. However, the POD model input data are the airfoil surface pressure readings instead of the full domain velocity readings. That's an alternative way to capture separation locations via pressure gradient values [4].

2.1 POD modeling

Let $\boldsymbol{P}_i(\boldsymbol{x},\boldsymbol{t}), i=1,2...,N$, represents the set of N snapshots of the pressure flow field variable at the location $\boldsymbol{x}=\boldsymbol{x}(x,y)$ ... The average value of these set of snapshots is calculated from:

$$\bar{\boldsymbol{P}} = \frac{1}{N}\sum_{i=1}^{i=N} \boldsymbol{P}_i(\boldsymbol{x},\boldsymbol{t}) \tag{1}$$

A new data set representing the pressure fluctuations or variation is:

$$\boldsymbol{Pv}_i = \boldsymbol{P}_i - \bar{\boldsymbol{P}} \tag{2}$$

An optimal compact description of the data in Eqn. 2 needs to be defined. According to Karhunen-Loeve expansion, such data set can be represented by the following series:

$$\boldsymbol{Pv}(\boldsymbol{x},\boldsymbol{t}) = \sum_{i=1}^{i=N_s} \boldsymbol{\alpha}_i(\boldsymbol{t})\,\phi_i(\boldsymbol{x}) \tag{3}$$

where N_s is the number of the modes used, $\boldsymbol{\alpha}_i(\boldsymbol{t})$ is the amplitude of each mode, and $\phi_i(\boldsymbol{x})$ is the eigenmode. In order to get the optimal set of the eigenmodes, ϕ , it requires that the basis functions (eigenmodes) to be the solution of the POD Fredholm integral equation:

$$\int \boldsymbol{C}(\boldsymbol{x},\boldsymbol{x}')\phi(\boldsymbol{x}')d\boldsymbol{x} = \lambda\phi(\boldsymbol{x}) \tag{4}$$

where $\boldsymbol{C}$ is a kernel calculated as follows:

$$\boldsymbol{C}(\boldsymbol{x},\boldsymbol{x}') = \frac{1}{N}\sum_{i=1}^{i=N} \boldsymbol{Pv}_i(\boldsymbol{x},\boldsymbol{t})\,\boldsymbol{Pv}_i(\boldsymbol{x}',\boldsymbol{t}) \tag{5}$$

where $\boldsymbol{C}(\boldsymbol{x},\boldsymbol{x}')$ is the data set averaged two-point $(\boldsymbol{x},\boldsymbol{x}')$ correlation matrix, $\boldsymbol{x}$ and $\boldsymbol{x}'$ are two distinct points, and N is the number of snapshots. Using the snapshots method so as to get the POD modes ϕ , an eigenvalue problem needs to be constructed:

$$\sum_{j=1}^{j=N} \boldsymbol{L}_{ij}\boldsymbol{\psi}_j = \lambda\boldsymbol{\psi}_i \tag{6}$$

where λ and $\boldsymbol{\psi}$ are the eigenvalues and eigenvectors of $\boldsymbol{L}$, respectively, and $\boldsymbol{L}$ is the correlation matrix defined by:

$$\boldsymbol{L}_{ij} = \frac{1}{N}(\boldsymbol{Pv}_i \cdot \boldsymbol{Pv}_j) = \frac{1}{N}\int \boldsymbol{Pv}_i \boldsymbol{Pv}_j^T d\boldsymbol{x} \tag{7}$$

where $(\boldsymbol{Pv}_i \cdot \boldsymbol{Pv}_j)$ represents the dot (inner) product and the superscript ^{T} indicates the transpose of variation pressure vector. It is noted that $\boldsymbol{L}$ is a symmetric positive definite matrix yielding real eigenvalues and orthogonal eigenmodes that represent a full set of solutions inside the data set space [16]. The eigenmodes ϕ are calculated as follows:

$$\phi_i = \sum_{i=1}^{i=N_s} \boldsymbol{\psi}_i \boldsymbol{Pv}_i(\boldsymbol{x},\boldsymbol{t}) \tag{8}$$

and $\boldsymbol{\alpha}_i(\boldsymbol{t})$ is calculated from:

$$\boldsymbol{\alpha}_i(\boldsymbol{t}) = \frac{\boldsymbol{Pv}_i(\boldsymbol{x},\boldsymbol{t})\cdot\phi_i}{\phi_i\cdot\phi_i} = \frac{\int \boldsymbol{Pv}_i(\boldsymbol{x},\boldsymbol{t})\phi_i^T d\boldsymbol{x}}{\int \phi_i\phi_i^T d\boldsymbol{x}} \tag{9}$$

To sum up, the POD model can be constructed by following the steps listed below:

1. Extract the pressure snapshots $\boldsymbol{P}_i$ (readings sets) from numerical or experimental methods.
2. Get the average pressure $\bar{\boldsymbol{P}}$ flow field parameter using Eqn. 1.

3. Get the pressure variance $\boldsymbol{Pv}_i$ using Eqn. 2.
4. Compute the correlation matrix $\boldsymbol{L}_{ij}$ using Eqn. 7.
5. Get the eigenvalues $\boldsymbol{\lambda}$ and eigenvectors $\boldsymbol{\psi}_i$ by solving Eqn. 6.
6. Get the basis functions $\boldsymbol{\phi}_i$ using Eqn. 8.
7. Get the mode value $\boldsymbol{\alpha}_i(\boldsymbol{t})$ using Eqn. 9.
8. Reconstruct the pressure $\boldsymbol{Pv}(\boldsymbol{x},\boldsymbol{t})$ flow field parameter using Eqn. 3.

The approximation degree of the data set solution $\boldsymbol{P}(\boldsymbol{x},\boldsymbol{t})$ (the respect to $\boldsymbol{P}_{N_s}(\boldsymbol{x},\boldsymbol{t})$ (the reconstructed solution by POD using N_s modes), by checking how their ratio, E_N, is CFD solution) can be measured with near to unity:

$$E_N = \frac{\sum_{i=1}^{i=N_s} \boldsymbol{\lambda}_i}{\sum_{i=1}^{i=N} \boldsymbol{\lambda}_i} \tag{10}$$

The above expression can also be used to show the relative energy associated with a specific mode to the total system energy. As proven by Sirovich [17], the POD expansion is optimal in the minimization of the mean square error between the full data set and its reconstruction, and required modes number describing the data set for a certain error as well.

3. Modified linear stochastic measurement

It's a method used to represent flow field alongside the POD method. The Modified Linear Stochastic Measurements (MLSM) method simply is as follows: Given one of the variables of the flow field at some few points; the flow field for the whole domain can be reconstructed. In the previous section, it's shown that the POD method represents the flow field by two series functions; a space series function $\boldsymbol{\phi}(\boldsymbol{x})$ and a time series function $\boldsymbol{\alpha}(\boldsymbol{t})$. In this section, the MLSM method yields the value of $\tilde{\boldsymbol{\alpha}}_n(\boldsymbol{t})$ by measuring pressure at this time at various distinct locations. Using the airfoil surface pressure only, MLSM technique provides the ability to predict the flow state around the airfoil for all the time domain. Compared to the POD technique in the calculation of the time expansion coefficient, MLSM is characterized by its speed, accurate results with fewer calculations, and better memory savings [4].

3.1 MLSM formulation

The low-dimensional flow time expansion coefficient $\tilde{\boldsymbol{\alpha}}_n(\boldsymbol{t})$ can be directly measured from a few number of sensors or CFD computed pressure readings located on the airfoil surface. Using these instantaneous pressure readings $\boldsymbol{P}_i(\boldsymbol{t})$ at each streamwise location i on the airfoil surface, the estimated POD time expansion coefficient can be describes as series expansion per each POD mode n as follows [18]:

$$\begin{aligned}\tilde{\boldsymbol{\alpha}}_n(t) &= \boldsymbol{A}_{ni}\boldsymbol{P}_i(t) + \boldsymbol{B}_{nij}\boldsymbol{P}_i(t)\boldsymbol{P}_j(\boldsymbol{t}) \\ &+ \boldsymbol{C}_{nijk}\boldsymbol{P}_i(\boldsymbol{t})\boldsymbol{P}_j(\boldsymbol{t})\boldsymbol{P}_k(\boldsymbol{t}) + \ldots \\ &\qquad i,j,k \in [1,q]\end{aligned} \tag{11}$$

where $\tilde{\boldsymbol{\alpha}}_n(\boldsymbol{t})$ is the mode value using MLSM method or any higher order and q is the number of the used pressure sensors (reading points). By applying truncation to the above series non-linear terms, we could obtain a simplified expression for $\tilde{\boldsymbol{\alpha}}_n(\boldsymbol{t})$ [4]:

$$\tilde{\boldsymbol{\alpha}}_n(\boldsymbol{t}) = \boldsymbol{A}_{ni}\boldsymbol{P}_i(\boldsymbol{t}) + O[\boldsymbol{P}_i^2(\boldsymbol{t})] \tag{12}$$

The MLSM coefficients $\boldsymbol{A}_{ni}$ are chosen in a way to minimize the mean squared error $\boldsymbol{e}_{\tilde{\alpha}_n}$ which is defined as:

$$\boldsymbol{e}_{\tilde{\alpha}_n} = \overline{[\tilde{\boldsymbol{\alpha}}_n(\boldsymbol{t}) - \boldsymbol{\alpha}_n(\boldsymbol{t})]^2} = \overline{[\boldsymbol{A}_{ni}\boldsymbol{P}_i(\boldsymbol{t}) - \boldsymbol{\alpha}_n(\boldsymbol{t})]^2} \tag{13}$$

and by applying minimization condition $\frac{\partial \boldsymbol{e}_{\tilde{\alpha}_n}}{\partial \boldsymbol{A}_{ni}} = 0$.

It follows that it can be represented as a linear system of equations of matrix size q in the unknowns vector $\boldsymbol{A}_{ni}$ as follows:

$$\begin{bmatrix} \langle \boldsymbol{P}_1^2 \rangle & \langle \boldsymbol{P}_1\boldsymbol{P}_2 \rangle & \cdots & \langle \boldsymbol{P}_1\boldsymbol{P}_q \rangle \\ \langle \boldsymbol{P}_2\boldsymbol{P}_1 \rangle & \langle \boldsymbol{P}_2^2 \rangle & \cdots & \langle \boldsymbol{P}_2\boldsymbol{P}_q \rangle \\ \vdots & \vdots & \ddots & \vdots \\ \langle \boldsymbol{P}_q\boldsymbol{P}_1 \rangle & \langle \boldsymbol{P}_q\boldsymbol{P}_2 \rangle & \cdots & \langle \boldsymbol{P}_q^2 \rangle \end{bmatrix} \begin{bmatrix} \boldsymbol{A}_{n1} \\ \boldsymbol{A}_{n2} \\ \vdots \\ \boldsymbol{A}_{nq} \end{bmatrix} = \begin{bmatrix} \langle \boldsymbol{\alpha}_n\boldsymbol{P}_1 \rangle \\ \langle \boldsymbol{\alpha}_n\boldsymbol{P}_2 \rangle \\ \vdots \\ \langle \boldsymbol{\alpha}_n\boldsymbol{P}_q \rangle \end{bmatrix} \tag{14}$$

By solving the linear system in Eqn. 14, the MLSM coefficients can be extracted then substituted in Eqn. 12 to get the estimated POD coefficients. Next, the estimated pressure distribution over the airfoil can be reconstructed by combining the POD eigenfunctions $\boldsymbol{\phi}_i(\boldsymbol{x})$, that were calculated earlier, with the estimated POD coefficients $\boldsymbol{\alpha}_i(\boldsymbol{t})$ by rewriting Eqn. 3 as follows:

$$\tilde{\boldsymbol{Pv}}(\boldsymbol{x},\boldsymbol{t}) = \sum_{n=1}^{n=N_s} \tilde{\boldsymbol{\alpha}}_n(\boldsymbol{t})\boldsymbol{\phi}_n(\boldsymbol{x}) \tag{15}$$

4. Results and discussions

4.1 MLSM formulation

In this section, the OpenFOAM®'s CFD solution of the air flow over a DU-96-W-180 airfoil, obtained by Halawa [19], is compared with the reconstructed POD solution using different number of modes Ns where the maximum $N_s = 30$. The different factors affecting the reconstructed POD solution are shown and discussed. Besides, the distribution of the POD modes, eigenvalues, and the captured energy by using different number of modes are shown. Thereafter, using different number of modes, the POD modes and their corresponding solutions (reconstruction of the flow) are presented and compared to the CFD solution showing the error difference. The POD procedure was executed by implementing a

MATLAB® subroutine whose results are discussed as follows. The relative energy associated with each of the first five modes is bar graphed in Fig. 1. It clearly shows that only the first few POD modes possess the main energy of the system.

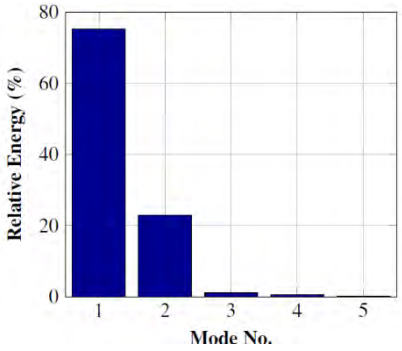

Fig. 1: Relative energy of POD modes.

Alternatively, Fig. 2 also verifies that using only 3 POD modes can capture most of the system energy up to 99%, while the first mode only possesses around 75%. Thereby the POD is a powerful tool for getting reduced order solution with only few number of modes (i.e. few calculations).

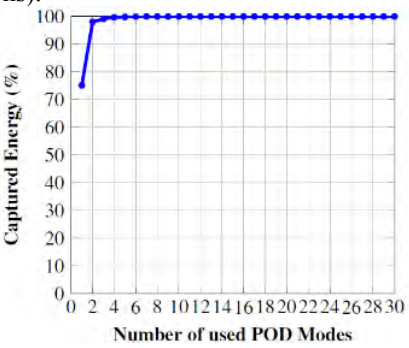

Fig. 2: Captured energy with the number of used POD modes

The log of the eigenvalues of the POD modes are shown in Fig. 3. It can be observed from that the first mode has the highest eigenvalue. Besides, as the number of eigenmodes increases their corresponding eigenvalues are nearly zero. Thus, Fig. 3 confirms that the solution can be reconstructed using few number of POD modes.

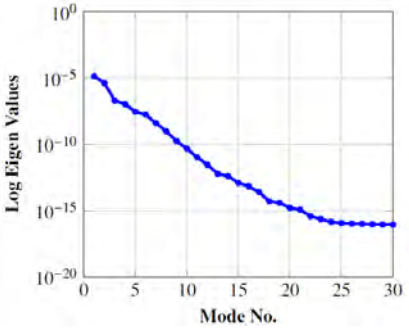

Fig. 3: Log of eigen values with the number of used POD modes

The first four pressure POD modes functions of the flow around the airfoil are shown in Fig. 4. It is obvious that the first mode function is the dominant mode mapping the usual pressure distribution with maximum energy content (physical representation). The second mode shows different distribution (less energy content/amplitude) when combined with the first one will yield more accurate resultant pressure distribution. The rest of the modes starting from the third mode are clearly of low impact on the pressure distribution verifying Fig. 1 as expected. Furthermore, considering the pressure gradient of each mode, the first mode showed the highest gradient so it had the dominant effect on flow separation. Thus, first-mode is sufficient to predict separation and should be considered for future feedback control.

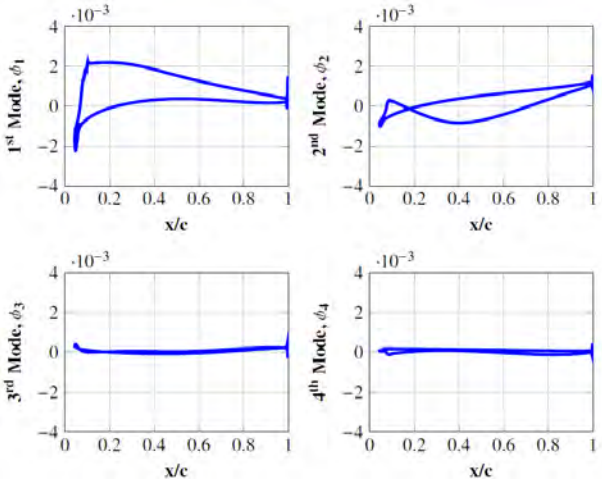

Fig. 4: Pressure POD mode functions distribution of flow around the airfoil

The variation of the amplitude of each of the first four POD modes with the non-dimensional time, $\bar{t}$ is presented in Fig. 5. The non-dimensional is defined here as the actual time divided by L / U_∞ which is equal to 100 in this case, where, L is the airfoil chord length and U_∞ is the flow velocity. The calculations were done here using Eqn. 9. It can be concluded from Fig. 5 that as the mode number increases the frequency of the corresponding amplitude increases. Thus, accompanied by the results in Fig. 4, the highest impact on the flow field results from the first mode.

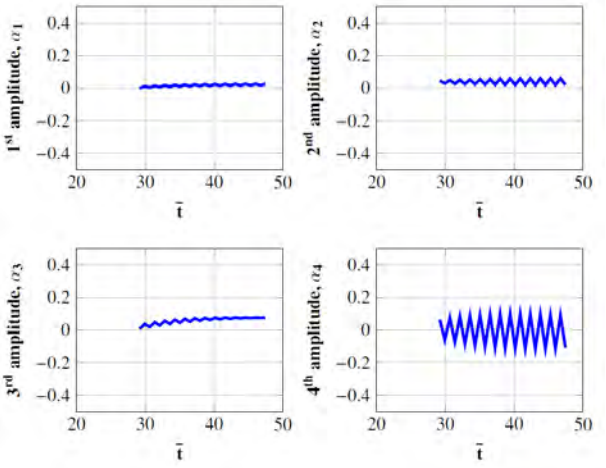

Fig. 5: Variation of the amplitude of each POD mode with the non-dimensional time

The reconstruction of the average pressure field was done using Eqn. 3. Fig. 6 shows a comparison between the CFD solution obtained from OpenFOAM® and the POD reconstructed solution for the pressure coefficient distribution, C_p, defined in Eqn. 16, using one, two, three, and four POD modes in the expansion of Eqn. 3. The one-POD-mode solution shows a very similar solution to the CFD solution because of the high-energy content however with some deviation due to missing energy portion (around 25%). The two-POD-mode solution shows more promising results with much higher accuracy that the first mode only. Starting from three-POD-mode solution, the results are matching the CFD solution due to achieving near the 99% of the energy content.

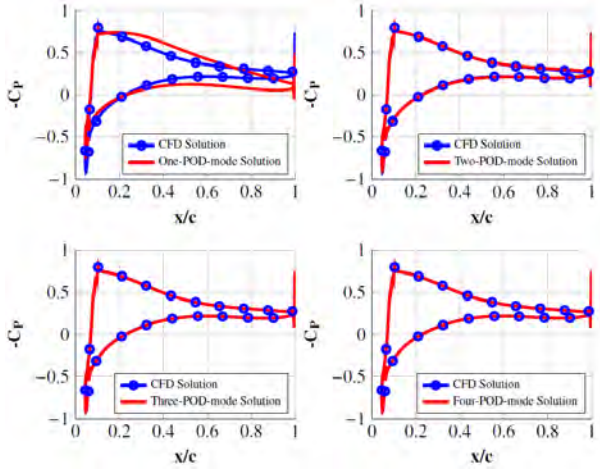

Fig. 6: Comparison between CFD solution and POD solution using different number of POD modes

$$C_P = \frac{P - P_\infty}{\frac{1}{2}\rho(U_\infty)^2} \qquad (16)$$

Furthermore, some small pressure spikes were encountered near the minimum pressure point due to the usual formation of small separation bubble near this region. Thus, this region possess some sort of flow dynamic instability affecting the surface pressure values at this location. The root mean squared error, RMSE of the reconstructed POD solution with respect to OpenFOAM® CFD solution is shown in Fig. 7 by checking different accuracy levels (i.e. mode numbers) at the first non-dimensional time $\bar{t} = 1$. The RMSE is computed from Eqn. 17 by taking the square root of the mean of the squares of the error between the two solutions for all points along the airfoil surface with respect to the mean of the original CFD solution.

$$RMSE = \frac{\sqrt{Mean(|P_{POD} - P_{CFD}|^2)}}{Mean(P_{CFD})^2} \qquad (17)$$

From Fig. 7, it is verified that the error decreases drastically when using 2 POD modes and more. It confirms the convenience of the POD method in obtaining accurate solutions using few calculations.

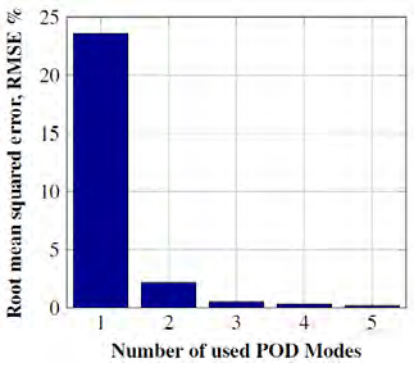

Fig. 7: RMSE variation with the number of used POD modes

4.2 MLSM formulation

In this section, the MLSM is applied to the OpenFOAM®'s CFD solution of the flow around a DU-96-W-180 airfoil, obtained by Halawa [19], to check the accuracy of estimating the time expansion coefficient $\tilde{a}_n(t)$ by using only the pressure readings from the probes (sensors) on the surface of the airfoil. Next, numerical results are presented for the MLSM technique by measuring the estimated time expansion coefficient $\tilde{a}_n(t)$ directly and comparing it with the POD time expansion coefficients $a_n(t)$ calculated earlier rather than reconstructing the pressure field variable. The MLSM results are shown for 20 pressure sensors which are distributed, as in Fig. 8a, at equidistant points on the airfoil surface along the chord line (x-axis) spanning the region from the separation bubble till the separation wake zone. Sensitivity study is held for the influence of the number of the pressure sensors used and their locations in the following section.

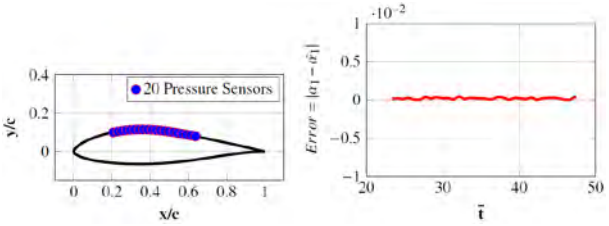

(a) (b)

Fig. 8: Sensitivity study using 20-sensors. (a) Sketch of airfoil DU-96-W-180 and 20-sensor locations. (b) Error distribution between the first mode of POD and MLSM for 20 pressure sensors

According to the results of the POD study earlier, it was clear that the dominant modes are the first few modes. Thus, in this study, the first mode coefficient (captures 75 % of the total system energy) is being investigated for both POD and MLSM methods. Fig. 8b shows the error distribution between the first mode of POD and MLSM corresponding to the 20 sensor locations in Fig. 8a.

4.2.1 Sensitivity study for sensors number and location

In this section, the influence of the number of the used pressure sensors and their locations along the airfoil surface on the estimated time expansion coefficient $\alpha_1(t)$ was investigated. Obviously, as shown from previous results, the magnitude of the pressure fluctuations downstream of the airfoil, as the separation wake region is approached, is larger than its upstream value. Consequently, it could be predicted that the pressure reading sensors downstream will represent the flow effectively during the MLSM calculation of $\alpha_1(t)$. Fig. 9a to Fig. 9d show the sensors locations and error distribution using 2 pressure sensors points for upstream and downstream cases, respectively. Besides, Fig. 9e and 9f shows one-upstream and one-downstream sensors locations and error distribution, respectively.

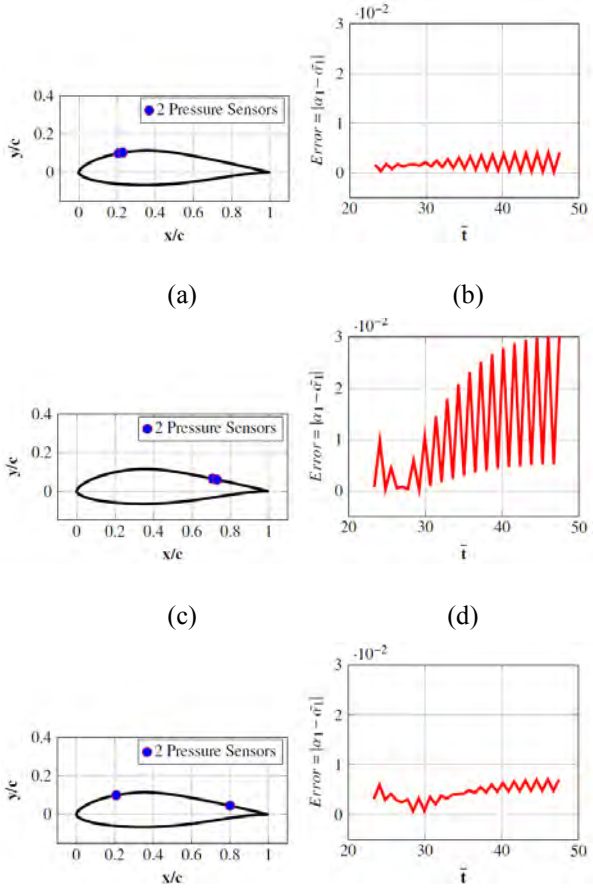

Fig. 9: Sensitivity study using 2-sensors. (a) 2-upstream, (c) 2-downstream, (e) 1-upstream and 1- downstream. (b), (d), and (f) Corresponding error distribution between the first mode of POD and MLSM for 2 pressure sensors located at (a), (c), and (e) respectively.

Next, the number of the sensor locations was increased from 2 to 10 and the $\alpha_1(t)$ distribution was checked. Similarly, Fig. 10a to Fig. 10d show the sensors locations and $\alpha_1(t)$ distribution using 10 pressure sensors points for upstream and downstream cases, respectively.

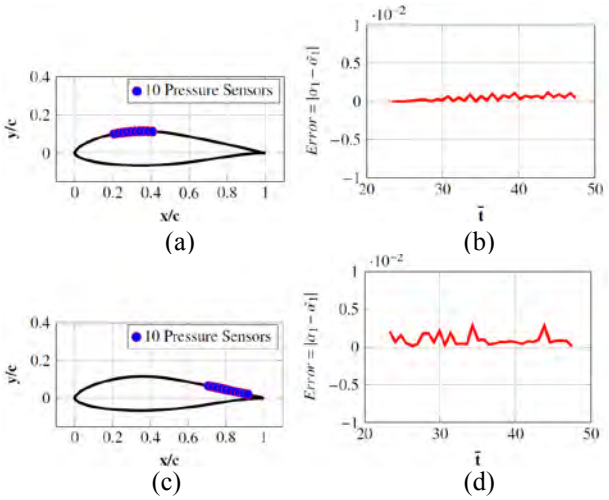

Fig. 10: Sensitivity study using 10-sensors. (a) 10-upstream, (c) 10-downstream. (b) and (d) Corresponding error distribution between the first mode of POD and MLSM for 10 pressure sensors located at (a) and (c) respectively.

In conclusion, the previous sensitivity study shows that the downstream pressure sensors give accurate result only after increasing the number of sensors from 2 to 10. Besides, Fig. 8b with 20 pressure sensors shows the best accuracy of all presented cases. It shows great agreement between the POD results and MLSM ones for the same first mode value. Thus, it would represent the flow field accurately around the airfoil. Consequently, as the number of sensors increases, better accuracy is achieved. However, a more practical choice would settle on the case of 2 pressure sensors (one upstream and the other downstream), since it yields acceptable accuracy and would save much computations and experimental implications.

4.3 Flow control applications

One of the promising applications of the POD/MLSM method is the closed loop (feedback) active flow control (AFC). It's worth mentioning that AFC can be used in many applications to achieve drag reduction, lift enhancement, transition delay, separation postponement, mixing augmentation, flow-induced noise suppression, turbulence management ...etc. In wind energy field, active control of the blade flutter of wind turbines using aerodynamic control receives great attention recently. The role of the POD/MLSM method in the AFC is that it yields is a simplified governing equation for the flow that will aid in controlling the boundary layer separation in any feedback control application upon the block diagram shown in Fig. 11.

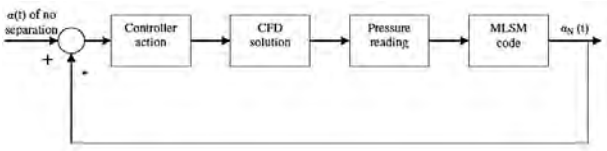

Fig. 11: Closed loop (feedback) active flow control block diagram [15].

The procedure involved in the above block diagram could be simply summarized as below:

- Reading the surface pressure distribution at each time step.
- Using MLSM method to get estimation of the dominant $\alpha_i(t)$ for which we can estimate the pressure field. From previous results, the first few coefficients have the largest amplitude, largest energy capturing and so largest impact in flow, so they are used as the controller input.
- The values of $\alpha_i(t)$ are compared with $\alpha_i(t)_{\text{no\_separation}}$ to get error as the controller input for feedback controller.
- Then the controller equation depends on the control technique.0 (e.g. excitation velocity = fn (error, gain, frequency, time)).

Regarding the computational time involved, the CFD solution for the case of Halawa [19], took around 6 hours on a Linux 12-core workstation. However, the POD/MLSM subroutine just took 2-3 seconds to compile and generate the physical solution with an acceptable accuracy. Thus, the reduction of the system dimensions will have a great impact on the feedback control time delay problem.

5. Conclusions

- The nature of aerodynamic flows yields non-linear unsteady partial differential equations whose computation requires numerical algorithms to be implemented on parallel massive super-computers which is a very complex task. Thus the essential need arises for other efficient tools to reducing the original complicated system of equations into a simple lower-dimensional model characterizing the physical process and capturing its behavior with relatively smaller number of degrees of freedom and lower computational cost.
- Using POD reduced order model had saved much computational time and expressed the flow field variables with high accuracy and less complexity. It was shown that using only 3 POD modes, most of the system energy could be captured (up to 99%) with RMS error less than 1%.
- Using POD in conjunction with MLSM technique was also efficient in achieving reduced order model using only few surface pressure readings. Using only 2 pressure sensors, one upstream and the other downstream, resulted in reasonable accurate solution.
- By increasing the number of pressure sensors (readings), the accuracy of MLSM increases. However, to be more practical, just few readings should be used with reasonable accuracy.
- Application of ROMs is important in reducing the computational time form several hours to just few seconds for applications involving recursive solution of the Navier-Stokes equations or any complex set of equations.
- Using the surface pressure values as an input to the POD/MLSM method instead of the whole velocity domain, is an efficient way to detect the locations of separation and apply the AFC effectively.
- The MLSM technique has a major impact in reducing the delay time in feedback control applications requiring recursive solution of complex sets of equations. This would be considered for future application in AFC.
- The extension of this application to whole blade and full wind turbine scale is an essential step to be addressed in the future work. Besides higher Reynolds numbers effect need to be investigated alongside various turbulence modeling.

References

[1] W. A. Silva, and P. S. Beran, Reduced-Order Modeling: New Approaches for Computational Physics. *AIAA Journal* (2001).

[2] G. Berkooz, P. Holmes, and J. Lumley, The Proper Orthogonal Decomposition in The Analysis of Turbulent Flows, *Annual Review of Fluid Mechanics* **25**, 1971, 539–575 (1993).

[3] J. L. Lumley, The structure of inhomogeneous turbulent flows, Atm. Turb. And Radio Wave Prop. (Yaglom and Tatarsky, ed.), Nauka, Moscow and Toulouse, France, 166–178, (1967).

[4] J. Ausseur, and J. Pinier, Toward Closed-Loop Feedback Control of the Flow Over NACA-4412 Airfoil, 43rd AIAA Aerospace Sciences Meeting, Reno, Nevada (2005).

[5] S. Siegel, K. Cohen, and T. McLaughlin, Feedback Control of a Circular Cylinder Wake in a Water Tunnel Experiment, 42nd AIAA Aerospace Sciences Meeting and Exhibit, Reno (2004).

[6] M. Luchtenburg, G. Tadmor, O. Lehmann, B. R. Noack, R. King, and M. Morzyński, Tuned POD Galerkin Models for Transient Feedback Regulation of the Cylinder Wake, 44th AIAA Aerospace Sciences Meeting, Reno, Nevada (2006).

[7] S. G. Siegel, K. Cohen, and T. McLaughlin, Numerical Simulations of a Feedback Controlled Circular

Cylinder Wake, *AIAA Journal* **44**(6), 1266–1276 (2006).

[8] J. Ausseur, J. Pinier, and M. Glauser, Flow Separation Control Using a Convection Based POD Approach, 3rd AIAA Flow Control Conference, San Francisco, California, 5-8 June, 2006.

[9] R. J. Adrian, On the role of conditional averages in turbulence theory, Turbulence in Liquids: *Proceedings of the Fourth Biennial Symposium on Turbulence in Liquids*, 323–332, (1977).

[10] D. R. Cole, M. N. Glauser, and Y. G. Guezennec, An Application of Stochastic Estimation to the Jet Mixing Layer, *Phys. Fluids* **4**(1), 192–194 (1991).

[11] J. P. Bonnet, D. R. Cole, J. Delville, M. N. Glauser, and L. S. Ukeiley, Stochastic estimation and proper orthogonal decomposition: Complementary techniques for identifying structure, *Experiments in Fluids* **17**, 307–314 (1994).

[12] R. Schmit, and M. Glauser, Low Dimensional Tools for Flow-Structure Interaction Problems: Application to Micro Air Vehicles, 41st AIAA Aerospace Sciences Meeting and Exhibit (2003).

[13] R. Schmit, and M. Glauser, Improvements in Low Dimensional Tools for Flow-Structure Interaction Problems: Using Global POD, 42nd AIAA Aerospace Sciences Meeting and Exhibit (2004).

[14] M. N. Glauser, M. J. Young, H. Higuchi, and C. E. Tinney, POD Based Experimental Flow Control on a NACA-4412 Airfoil(Invited), 42nd AIAA Aerospace Sciences Meeting and Exhibit, Reno (2004).

[15] M. I. El-desouky, Flow Control for Circular Cylinder Using Proper Orthogonal Decomposition, Master's thesis, Cairo University, (2009).

[16] H. E. Khalifa, B. Elhadidi, and J. F. Dannenhoffer III, Efficient Coupling of Multizone and CFD Indoor Flow Models through Proper Orthogonal Decomposition, *ASHRAE Transactions* **113**, 2 (2007).

[17] L. Sirovich, Turbulence and the dynamics of coherent structures. I–Coherent structures. II-Symmetries and transformations. III - Dynamics and scaling, *Quarterly of Applied Mathematics* **45**, 561–571 (Oct. 1987).

[18] J. Pinier, J. Ausseur, M. N. Glauser, and H. Hiroshi, Proportional Closed-Loop Feedback Control of Flow Separation, *AIAA Journal* **45** (2007).

[19] A. M. Halawa, Active Control for Airfoil with Smart Slat, Master's thesis, Cairo University, (2016).